Acoustic emission modeling for crack extension detection using extended finite element method

Kuanfang He[1,2] Qinghua Lu[1]
1.School of Mechatronics Engineering
Foshan University
Foshan, China
2. Hunan Provincial Key Laboratory of Health Maintenance for Mechanical Equipment
Hunan University of Science and Technology
Xiangtan, China
hkf791113@163.com, qhlu@qq.com

Yanfeng Peng
Hunan Provincial Key Laboratory of Health Maintenance for Mechanical Equipment
Hunan University of Science and Technology
Xiangtan, China
pyf1988@sina.com

***Abstract*—The extended finite element method (XFEM) is implemented to model and solve acoustic emission (AE) response of an elastic plate with a crack extension. The numerical cases of AE signals propagation by different crack lengths are investigated, of which time-frequency characters of AE signals by wavelet transform are consistent with theoretical results. The ratio of time-frequency energy as a characteristic parameter is also studied for crack length identification. The ratio of time-frequency energy is proved to be a sensitive numerical parameter for quantitative prediction of crack length.**

Keywords-component; Acoustic emission modeling; XFEM; Crack extension; Time-frequency characters; Detection

I. INTRODUCTION

On many occasions, many defects such as cracks the fracture occur inside the structure, which are very difficult to be visually observed. The crack dynamics occur inside the structure results in generation of the high frequency elastic waves because of the release of stored elastic energy [1, 2]. These high frequency elastic wave can be detected by AE sensor [3, 4], which is known as AE detection technology. The AE detection technology is a non-destructive testing method for the health monitoring of the structure [5]. The sequence of AE signals passing from elastic waves by a crack up to the AE transducer contains the subject of the guided waves propagation studies [6, 7].

AE signal propagation can be treated as guided waves to examine structure. It is very difficult or even impossible for solving such problem of elastic wave propagation by analytical solution [8,9]. There are major numerical methods for wave simulation by the finite difference method, the boundary finite method and the finite element method[10-13]. Among the numerical methods for wave simulation, the finite element method has the primary advantage by the available codes, user friendly, and powerful function of sophisticated pre-and post-processing. The finite element method has been proved to be a good solution approach to the problem of guidance waves propagated in the structure with crack [14-17]. In the analysis of the fracture mechanics problem, the finite element method is limited, the defects are simplified and straight cracks, notches or cylindrical holes are used to represent real cracks. The accuracy and effect of the solutions computed by FE model is mesh-dependent.

In modeling of crack, the XFEM has a unique advantage in wave propagation caused by crack extension [18, 19]. The XFEM provides flexibility and versatility in crack modeling based on the enrichment of the FE model with additional degrees of freedom. In addition, previous literatures [20, 21] used the XFFE method to numerically calculate wave propagation in a plate. The crack extension is presented by the moment tensor that is considered as boundary condition on the crack surface. The AE signal of crack extension is calculated by XFFE, of which the numerical cases by different crack lengths are investigated for detection.

The paper is organized as follows. In Section 2, the wave equation and the boundary conditions for an elastic plate structure with a crack extension are discussed. In Section 3, we show the modeling and solution of the problem of an elastic plate structure with a crack extension by XFEM. In Section 4, the calculated results are discussed. At last, the conclusions are summarized.

II. ACOUSTIC EMISSION WAVE EQUATION OF THE CRACK EXTENSION

For a plate structure containing a rectangular cross-section straight crack, the crack extension in the unit on the plate width is assumed to be uniform. Thus, the three-dimensional problem of elastic dynamical displacement field of plate structure caused by crack extension can be reduced to two-dimensional model, the schematic is represented in Fig. 1.

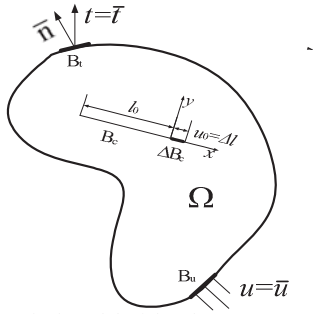

Figure1. Elastic dynamical model of the plate structure with a crack extension

978-1-7281-0860-5/19/$31.00 ©2019 IEEE

$\Omega \in R_2$ and piecewise smooth boundary B are considered as A cracked body with open initial domain. $B_u \cup B_t \cup B_c \cup \Delta B_c = B$. t represents stress, u represents displacement, B_t represents stress boundary, B_u represents displacement boundary, B_c represents the crack surface, ΔB_c represents the crack extension surface with length of Δl. In absence of body and traction force, the problem of displacement field function $u(x, y, t)$ is solved by satisfying the governing equations by(1)-(3).

$$\nabla \cdot \sigma - \rho \ddot{u} = 0 \tag{1}$$

$$\varepsilon = \nabla_s u \tag{2}$$

$$\sigma = D : \varepsilon \tag{3}$$

The symbol ∇ is the spatial gradient operator, $\ddot{u}$ is the acceleration of mixture, and ρ is the total density. The displacement is $\boldsymbol{u}$, the strain tensor is ε, the stress tensor is σ and the isotropic fourth-order Hooke tensor is $\boldsymbol{D}$, ∇_s is the symmetric gradient operator on a vector field. According to the previous crack acoustic emission source model [22], crack propagation can be represented by the source moment tensors m_{pq}. Crack extension causes the displacement of the resilient body, which should satisfy the conditions as following.

Boundary condition of the initial displacement:

$$B_u: \ u = \overline{u} \tag{4}$$

Boundary condition of Initial stress:

$$B_t: \ \sigma.n = \overline{t} \tag{5}$$

Crack surface boundary condition:

$$B_c: \ t_0 = 0 \tag{6}$$

$$\Delta B_c: \ \sigma_{pq} = m_{pq} \tag{7}$$

The XFEM is proposed to solve the above problems.

III. The XFEM Formulation of Governing Equations

In order to derive the weak form of (1), the trial functions $u(X,t)$ and the test functions $\delta u(X,t)$ are required to be smooth enough to satisfy all essential boundary conditions and define the derivatives of equations. To obtain the weak form of governing equations, the test functions $\delta u(X,t)$ is multiplied by (3), and integrated over the domain Ω as

$$\int_{\Omega} \delta u \left(\nabla \cdot \sigma - \rho \ddot{u} \right) d\Omega = 0 \tag{8}$$

The weak form of governing equations can be obtained by expanding (8) and applying the Divergence theorem.

$$\int_{\Omega} \delta u \cdot \rho \ddot{u} d\Omega + \int_{\Omega} \nabla \delta u : \sigma d\Omega - \int_{\Delta B_c} \delta u \cdot \sigma_{pq} dB = 0 \tag{9}$$

The spatial and time domain discretization of (9) is derived by XFEM and the generalized Newmark.

A. Approximation of displacement Fields

The variable $\varphi(x,t)$ is approximated by the enhanced trial function $\varphi^h(x,t)$ as following [23].

$$\varphi(X,t) \approx \varphi^h(X,t) = \sum_{I \in N} N_I(X) \overline{\varphi}_I(t) + \sum_{J \in N^{dis}} N_J(X) \psi(X) \overline{a}_J(t) \tag{10}$$

where N is the all nodal points, $N_I(X)$ is the standard shape function, $\psi(X)$ denotes the Heaviside enrichment function. In order to achieve the Kronecker property of standard FEM shape functions, that is, $\varphi(X_J) = \varphi_J$ at the nodal point J. Equation (10) can be rewritten as follows.

$$\varphi(X,t) \approx \varphi^h(X,t) = \sum_{I \in N} N_I(X) \overline{\varphi}_I(t) + \sum_{J \in N^{dis}} N_J(X) \left(\psi(X) - \psi(X_J) \right) \overline{a}_J(t) \tag{11}$$

where $\psi(X)$ is defined for the strong discontinuity based on the Heaviside step function $H(x)$.

$$\psi(X) = H(X) = \begin{cases} +1 & if \ (X - X^*) \cdot n_d \geq 0 \\ 0 & otherwise \end{cases} \tag{12}$$

where X^* is the point on the discontinuity that is the closest distance from x. n_d is the unit normal vector to the discontinuity at point X^*.

Applying (11), the trial functions $u(X,t)$ can be defined as follows.

$$u(X,t) \approx u^h(X,t) = \sum_{I \in N} N_{ul}(X) \overline{u}_I(t) + \sum_{J \in N^{dis}} N_{uJ}(X) (H(X) - H(X_J)) \overline{a}_J(t) \tag{13}$$

where $\overline{a}_J$ is the additional DOF according to enrichment functions. N_u is the standard shape function of displacement field. The enriched *FE* approximation of the displacement (13) can be symbolically written as following.

$$u^h(X,t) = N_u^{std}(X) \overline{u}(t) + N_u^{Hev}(X) \overline{a}(t) \tag{14}$$

where $N_u^{std}(X)$ is the matrix of standard displacement shape function, N_u^{Hev} is the matrices of enriched displacement shape functions.

B. The XFEM Spatial discretization

Applying the trial functions of enriched displacement fields (11), the discredited form of integral equations (9) can be obtained according to the Bubnov-Galerkin technique as follows.

$$\begin{pmatrix} M_{uu} & M_{ua} \\ M_{au} & M_{aa} \end{pmatrix} \begin{Bmatrix} \ddot{\overline{u}} \\ \ddot{\overline{a}} \end{Bmatrix} + \begin{pmatrix} K_{uu} & K_{ua} \\ K_{au} & K_{aa} \end{pmatrix} \begin{Bmatrix} \overline{u} \\ \overline{a} \end{Bmatrix} - \begin{Bmatrix} f_u^{ext} \\ f_a^{ext} \end{Bmatrix} = 0 \tag{15}$$

where the matrices $\boldsymbol{M}$, $\boldsymbol{K}$ and external laod $\boldsymbol{f}$, and g are defined as

$$\begin{aligned} M_{\alpha\beta} &= \int_{\Omega} (N_\mu^\alpha)^T \rho N_\mu^\beta d\Omega \\ K_{\alpha\beta} &= \int_{\Omega} (B_\mu^\alpha)^T D B_\mu^\beta d\Omega \\ f_\alpha^{ext} &= \int_{\Delta B_c} (N_\mu^\alpha)^T \sigma_{pq} dB \end{aligned} \tag{16}$$

$(\alpha,\beta)\in(u^{std},a^{Hev})$ denote the "standard", "Heaviside" functions of the displacement field. The Newmark method is used to integrate the differential equations (15) in time [23].

IV. Numerical Results and Discussion

A. Modeled AE Signal Database

Considering the crack extension in the unit on the plate width is assumed to be uniform, the three-dimensional problem of elastic dynamical displacement field of plate structure caused by crack extension can be reduced to two-dimensional model. The thickness and length of plate is 10 mm and1000 mm respectively, the crack length is l_0, and extension length is Δl_0. Displacement $u_y(t)$ of the y direction is monitored at a point in the plate surface with distance of 200 mm to the crack position, which is shown in Fig.2.

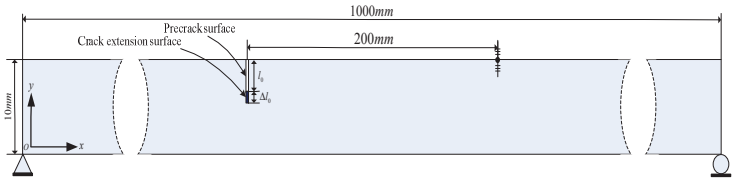

Figure 2. Plate crack extension XFEM model

Plate elastic wave propagates mainly in the form of Lamb waves, which is multi-mode and dispersion characteristics. Lamb wave characteristics equation is Rayleigh-Lamb equation [8].

$$\left[\frac{\tan(qh)}{\tan(ph)}\right]^{\pm 1}=-\frac{4k^2pq}{\left(q^2-k^2\right)^2} \tag{16}$$

where, $p^2=\frac{\omega^2}{c_L^2}-k^2$, $q^2=\frac{\omega^2}{c_T^2}-k^2$. k is wave number. h is half thickness of the sheet. ω is the circular frequency. c_L is the P-wave velocity. c_T is the shear velocity.

Fig.3 is the zero-order anti-symmetric elastic wave (A0) and symmetric elastic wave (S0) of the group velocity dispersion curves. Fig.4 is a theoretical time frequency distribution curve of the S0 and A0 mode at wave propagation distance of 200mm. The maximum frequency f_{max} is concerned about 0.5MHz, the smallest wavelength λ_{min} is concerned about 5. 6mm. So, the solution to this problem requires an integration time step $\Delta t\le 0.1$ us and an element length $l_e\le 0.28$ mm. The set of the XFEM model is in Table I. The property of the material is given in Table II.

TABLE I Configuration of the XFEM model

Plate Thickness	Plate length	Element length	Number of elements	Time step
H=10mm	L=1000mm	l_e=0.1 mm	100 x 10000	0.05us

TABLE II Material Properties

Young's modulus	Poisson's ratio	Density	Compression wave	Shear wave	Rayleigh wave
200 x 10^3N/mm^2	0.29	7850kg/m^3	5778m/s	3142m/s	2909m/s

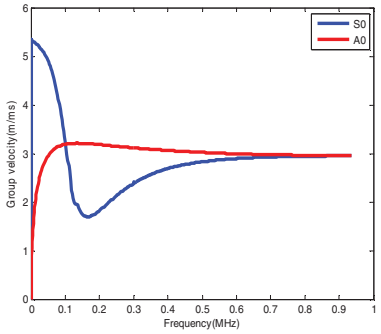

Figure 3. The group velocity dispersion curves (A0 and S0)

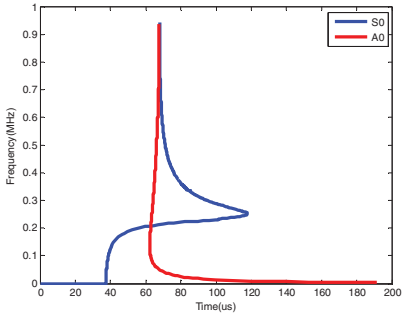

Figure 4. The theoretical time-frequency distribution curve under condition of propagation distance of 200mm

According to the above analysis, the acoustic emission source can be represented by an equivalent tensor on an infinitesimal element. So, the crack tip position is modeled by an element length, the tensor boundary in the x-and y-directions is imposed on the element. Fig.5(a) shows the applied tensor on the elements of the crack extension in the plate, and Fig.5(b) shows the time function of these tensor[8]. Crack extension length Δl_0 is 0.5mm, crack width is 0.1 mm, the crack extension unit size is applied to the surface with the uniform load $\lambda+2\mu$ and λ. The crack extension time is very short with rise time of 1.5us.

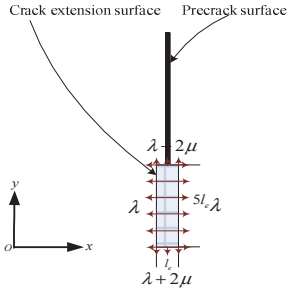

(a) The applied tensor as excitation of crack extension

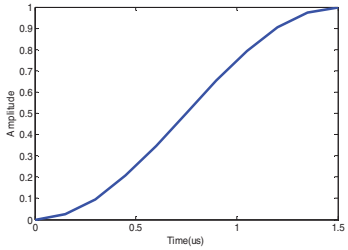

(b) The source-time function

Figure 5. The AE excitation source of the crack extension(mode I) in the plate

B.Time frequency analysis of AE signal

AE signal waveforms from crack extension lengths of 2.0 mm, 3.0 mm, 4.0 mm, 5.0 mm, 6.0mm, 7.0 mm and 8.0mm are calculated respectively. AE signal owns characteristics of transient and non-stationary, which cannot be fully described by analysis of time or frequency domain separately. The wavelet transform is performed to analyze AE signal waveform [24]. The Figs.6 (a)-12 (a) show the displacement versus time at *y*-direction after conducting the high pass filter of 40 kHz. Figs.6 (b)-12(b) are time frequency distributions of the AE signals. The theoretical time frequency distribution curves are also plotted in Figs.6 (b)-12 (b). As can be seem form the Figs.6 (b)-12(b), the time frequency distributions of the AE signals calculated by the XFEM are consistent with the theoretical ones, which are similar to the existing studies [25]. As also can be seem form the Figs.6(b)-12 (b), the AE signals are accompanied with some broadband frequency components, of which different frequencies components propagate at different speeds.

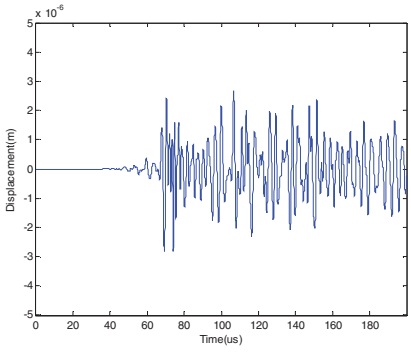

(a) AE signals waveform

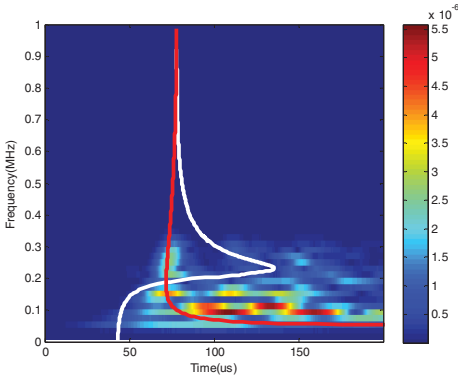

(b) time frequency distribution

Figure 6. The AE signals caused by the crack length of 2.0 mm

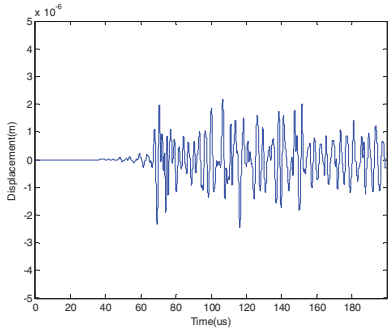

(a) AE signals waveform

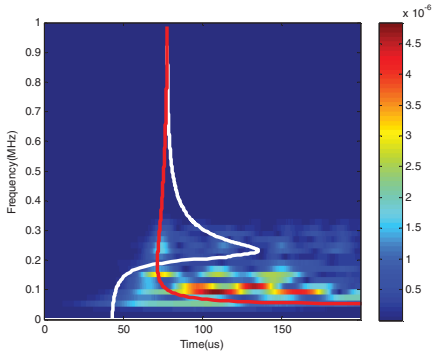

(b) time frequency distribution

Figure 7. The AE signals caused by the crack length of 3.0 mm

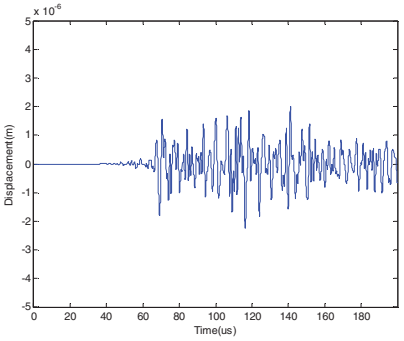

(a) AE signals waveform

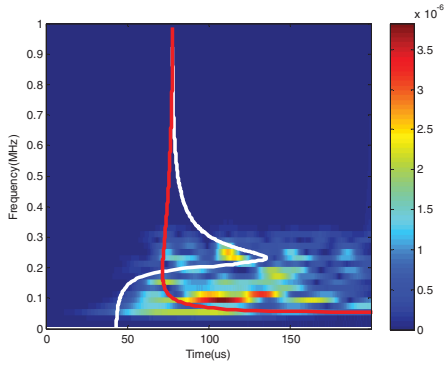

(b) time frequency distribution

Figure 8. The AE signals caused by the crack length of 4.0 mm

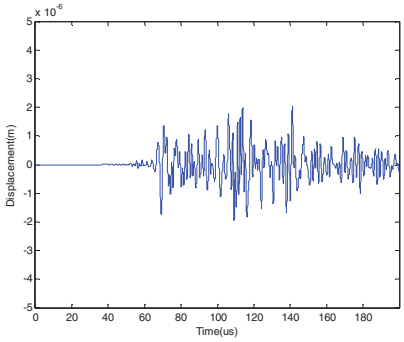

(a) AE signals waveform

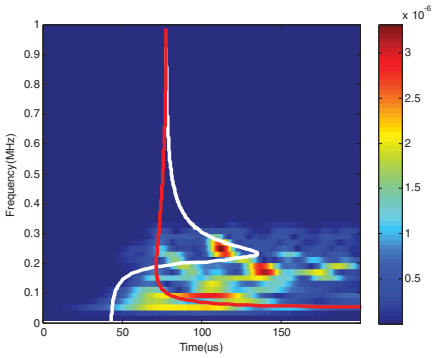

(b) time frequency distribution

Figure9. The AE signals caused by the crack length of 5.0 mm

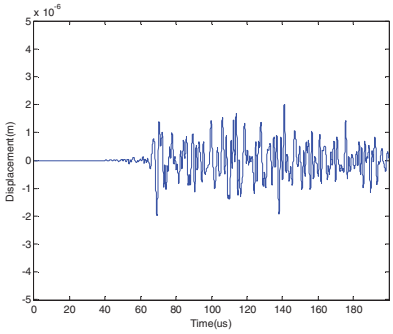

(a) AE signals waveform

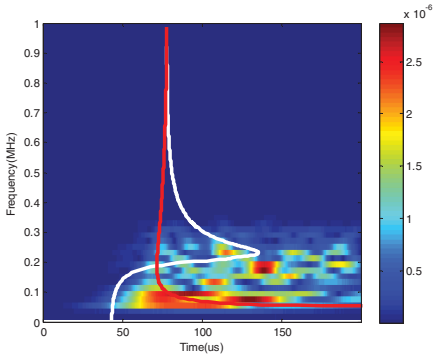

(b) time frequency distribution

Figure 10. The AE signals caused by the crack length of 6.0 mm

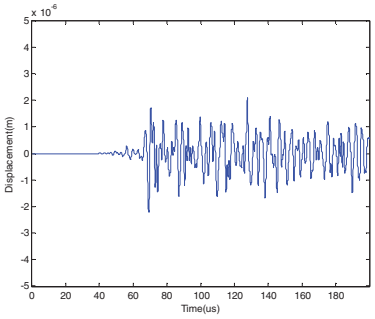

(a) AE signals waveform

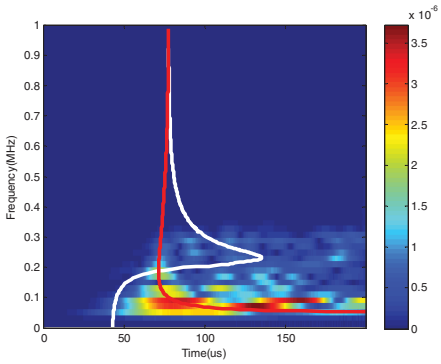

(b) time frequency distribution

Figure 11. The AE signals caused by the crack length of 7.0 mm

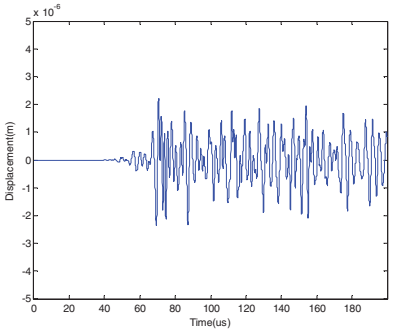

(a) AE signals waveform

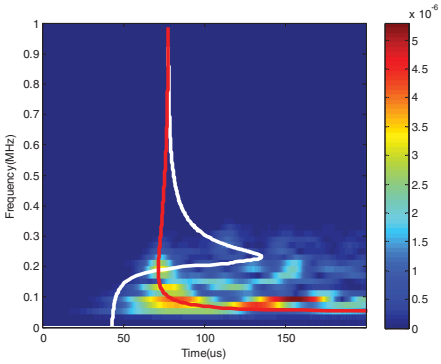

(b) time frequency distribution

Figure 12. The AE signals caused by the crack length of 8.0 mm

According to these figures, some observations indicate as following:

(1) Compared to the existing studies [25], the signal frequency components of this study are more complex at collection point as an increasing of time, which mainly dues to the reflection and interference impact of the crack surface.

(2) The amplitude of these AE signals are in the micron level, so the modal AE instrument must be broadband and very sensitive in the AE waveform detection.

(3) As can be seem form the Figs.6 (b)- 12(b), the A0 at low frequency is the main proportion in AE signal because the crack extension process in an asymmetrical state.

(4) The position of crack extension near the midplane of the plate structure has a more proportion for the S0 mode at 200-300 kHz.

C. Calculation of the energies of the AE signal for detection of crack extension length

The ratio of time-frequency energy of the A0 and S0 modes from different crack lengths is plotted in Fig.13.The energy ratio EA0/ES0 is a gradual decrease as an increasing of the crack lengths. The energy ratio has the smallest value when crack extension position at the midplane. It is also noted that energy ratio is increased when the crack length increases more than half of the plate. According to the regularity between the energy ratio and the crack length, identification of crack length can be achieved. If the monitored energy ratio EA0/ES0 is great, the crack should be determined on or near the plate surface. If the monitored energy ratio decreases continually, the crack should be determined by extending internally to the midplane in the plate structure. If the monitored energy ratio increases continually, the crack should be determined by extending internally over the midplane in the plate structure.

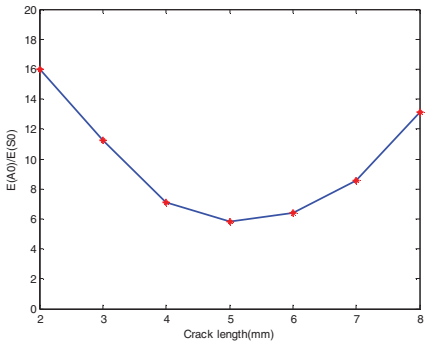

Figure13. The energy ratio EA0/ES0 from different crack lengths

V. CONCLUSIONS

The AE signal as guided waves is investigated by way of XFEM. The numerical cases are discussed as following.

(1) The numerical results show that time frequency characters of AE signal are consistent with the theoretical time frequency distribution curves. It demonstrates that the AE wave propagation characteristics by XFEM can meet certain accuracy by the choosing of a proper integration time step and mesh length.

(2) Identification of crack lengths can be achieved according to the ratio of time-frequency energy. If the monitored energy ratio is great, the crack should be determined on or near the plate surface. If the monitored energy ratio decreases continually, the crack should be determined by extending internally to the midplane in the plate structure. If the monitored energy ratio EA0/ES0 increases continually, the crack should be determined by extending internally over the midplane in the plate structure.

ACKNOWLEDGEMENTS

This work is supported by Hunan Provincial Natural Science Foundation of China under Grant 2017JJ1015, and National Natural Science Foundation of China under Grant 51475159 and 51805161, are gratefully acknowledged.

REFERENCES

[1] O. Y. Andreykiv, M. V. Lysak, O. M. Serhiyenko, et al, "Analysis of acoustic emission caused by internal cracks," Eng. Fract. Mech, vol. 68, no.11, pp.1317-1333, July 2001.

[2] A. Livne, E. Bouchbinder, I. Svetlizky, et al, "The Near-Tip Fields of Fast Cracks," Science, vol. 327, no. 5971, pp. 1359–1363, December 2010.

[3] M. J. Buehler, H. Gao, "Dynamical fracture instabilities due to local hyperelasticity at crack tips," Nature, vol. 439, no. 7074, pp. 307–310, January 2006.

[4] J. Fineberg, S. P. Gross, M. Marder, H.L. Swinney, "Instability in dynamic fracture," Phys. Rev, vol. 67, pp. 457–460, July 1991.

[5] C. Große, M. Ohtsu, "Acoustic Emission Testing in Engineering: Basics and Applications," Springer Verlag, Berlin, 2008.

[6] M.V. Lysak, Olexandr Ye, Andreykiv1, "Development of the theory of acoustic emission by propagating cracks in terms of fracture mechanics," Eng. Fract. Mech, vol. 55, no. 3, pp. 443–452, October 1996.

[7] J. D. Achenbach, "Wave propagation in elastic solids," J. Appl. vol. 41, no. 2, pp. 544, 1973.

[8] K. F. Graff, "Wave motion in elastic solids," J. Sound. Vibr, vol. 43, no. 4, pp. 721-722, December 1975.

[9] D. Alleyne, P. Cawley, "A two-dimensional Fourier transform method for the measurement of propagating multimode signals," J. Acoust. Soc, vol. 89, no. 3, pp. 1159–1168. September 1991.

[10] Wensheng Zhang, Fei Wu, "Finite Element Simulation of Acoustic Wave With Absorbing Boundary Conditions," IJACT, vol. 4, no. 23, pp. 626-634. 2012.

[11] W. Zhang, L.Tong and E. T. Chung, "Efficient simulation of wave propagation with implicit finite difference schemes," Numer. Math-Theory. Me, vol. 5, no. 22, pp. 205-228. 2012.

[12] G. Cohen, P. Joly, J. E. Robersts and N. Tordjman, "Higher order triangular finite elements with mass lumping for the wave equations," SIAM J. Numer, vol. 38, no. 6, pp. 2047-2078, July 2001.

[13] V. Etienne, E. Chaljub, J. Virieux and N. Glinsky, "An hp-adaptive discontinuous Galerkin finite-element for 3-D elastic wave modelling," Geophys. J, vol. 183, no. 4, pp. 941-962, Novermber 2010.

[14] M. J. S. Lowe, D. N. Alleyne and P. Cawley, "Defect detection in pipes using guided waves," Ultrasonics, vol. 36, pp. 147-154, February 1998.

[15] T. Vogt, M. Lowe and P. Cawley, "The scattering of guided waves in partly embedded cylindrical structures," J. Acoust. Soc, vol. 113, pp. 1258-1272, February 2003.

[16] B. Hosten and M. Castaings, "Finite elements methods for modelling the guided waves propagation in structures with weak interfaces," J. Acoust. Soc, vol. 117, pp. 1108-1113. March 2005.

[17] M. J. S. Lowe and O. Diligent, "Low-frequency reflection characteristics of the S0 Lamb wave froma rectangular notch in a plate," J. Acoust. Soc, vol. 111, pp. 64-74. January 2002.

[18] Menouillard T, Réthoré J, Combescure A, Bung H, "Efficient explicit time stepping for the extended finite element method (X-FEM)," Int. J. Numer. Meth. Eng, vol. 68, no. 9, pp. 911-939. April 2006.

[19] Menouillard T, Song J H, Duan Q, Belytschko T, "Time dependent crack tip enrichment for dynamic crack propagation," Int. J. Fracture, vol. 162, pp. 33–49, March 2010.

[20] S. Ham, Klaus-Jürgen Bathe, "A finite element method enriched for wave propagation problems," Comput Struct, vol. 94–95, pp. 1–12, March 2012.

[21] Zhanli Liua, Jay Oswaldb, Ted Belytschkoa, "XFEM modeling of ultrasonic wave propagation in polymer matrix particulate fibrous composites," Wave Motion, vol. 50, no. 3, pp. 389-401, April 2013.

[22] G. R. M. Sause, S. Richler, "Finite Element Modelling of Cracks as Acoustic Emission Sources," J. Nondestruct. Eval, vol.34, no.1, pp.1-13.February 2015.

[23] R. Amir. Khoei, "Extended Finite Element Method Theory And Applications. John Wiley & Sons," Ltd, 2015.

[24] F. L. D. Scalea, J. Mcnamara, "Measuring high-frequency wave propagation in railroad tracks by joint time–frequency analysis," J. Sound. Vibr, Vol. 273, pp. 637-651. June 2004.

[25] M. A. HAMSTAD, "Acoustic Emission Signals Generated By Monopole (Pencil lead break) Versus Dipole Sources: Finite Element Modeling And Experiments," J. Acoust, vol. 25, pp. 92-106. 2007.